(24) Summerfield, G. C.; Mildner, D. F. R. *J. Appl. Crystallogr.* **1983**, *16*, 384.
(25) Frank, F. C.; Keller, A.; Mackley, M. R. *Polymer* **1971**, *12*, 468.
(26) Pennings, A. J.; Schouteten, C. J. H.; Kiel, A. M. *J. Polym. Sci., Polym. Symp. Ed.* **1972**, *38*, 167.
(27) Kanamoto, T.; Tsuruta, A.; Tanaka, K.; Takeda, M.; Porter, R. S. *Polym. J.* **1983**, *15*, 327.
(28) Kanamoto, T.; Tsuruta, A.; Tanaka, K.; Takeda, M.; Porter, R. S. *Macromolecules* **1988**, *21*, 470.
(29) Cohen, Y.; Thomas, E. L. *Macromolecules* **1988**, *21*, 436.
(30) Flood, J. E.; White, J. L.; Fellers, J. F. *J. Appl. Polym. Sci.* **1982**, *27*, 2965.
(31) Hashimoto, T.; Todo, A.; Kawai, H. *J. Polym. Sci., Polym. Phys. Ed.* **1973**, *11*, 149.

Small-Angle Neutron Scattering from Star-Branched Polymers in the Molten State

J. C. Horton, G. L. Squires,* A. T. Boothroyd,† L. J. Fetters,‡ A. R. Rennie,§ C. J. Glinka,⊥ and R. A. Robinson‖

Cavendish Laboratory, Madingley Road, Cambridge CB3 0HE, U.K.
Received March 22, 1988; Revised Manuscript Received July 8, 1988

ABSTRACT: We have investigated the structure of a number of linear and star-branched polyethylene molecules, with arm numbers ranging from 3 to 18, by small-angle neutron scattering. Measurements were made in the melt at a temperature of 140 °C. Our measurements show that the Benoit scattering function, based on a random-walk model, gives an extremely good fit to the neutron scattering data, but the molecules are swollen with respect to a simple Gaussian conformation. The swelling is consistent with a model of an impenetrable core from which the arms of the star diffuse outward.

Introduction

The properties of branched polymers often differ markedly from those of linear polymers of the same molecular weight, and there is an obvious need to correlate the properties of these polymers with the type and degree of branching. Both natural and man-made samples of polymers often consist of mixtures of branched and unbranched molecules, with a wide range of molecular weights, frequency of branches, and segment length between branch points. Such diversity poses problems for interpreting the properties of the material, and theoretical models usually deal with simple branched structures. The simplest type of branching is that of star branching, where a number f of linear chains with equal numbers of monomers N are joined at a single branch point. We have measured the mean-squared radius of gyration $\langle S^2 \rangle$ by small-angle neutron scattering (SANS) for stars in the melt for a range of arm numbers and arm lengths.

It was suggested by Flory[1] in 1949 that linear polymers in the melt have a Gaussian or "random-walk" conformation. This was confirmed by SANS measurements in the early 1970s,[2] which showed that $\langle S^2 \rangle$ is proportional to N. However, it is to be expected that star molecules will show some departure from Gaussian behavior due to packing constraints near the branch point and that such departure will be most significant for molecules with a large number of short arms.

Experiment

The material used in our experiments was polyethylene. The stars were made in polybutadiene form by one of us (L.J.F.[3]). The arms were prepared, with low polydispersity ($M_w/M_n \approx 1.05$), by anionic polymerization. Polybutadiene prepared in this way has about 19 vinyl groups per thousand carbon atoms.[4] The star was formed by linking the arms to a chlorosilane core (Figure 1). From each polybutadiene star we prepared two forms of polyethylene by a catalytic reaction in which the double bond is saturated with either deuterium, to give a labeled molecule, or with hydrogen, to give an unlabeled molecule, thus

$$—[CH_2CH{=}CHCH_2—] + D_2 \rightarrow —[CH_2CHDCHDCH_2—]$$

$$—[CH_2CH{=}CHCH_2—] + H_2 \rightarrow —[CH_2CH_2CH_2CH_2—]$$

The process is described elsewhere.[5,6] After they were dried, the samples were tested for saturation by examining their infrared spectrum to check the absence of the 967-cm^{-1} absorption line. Doi et al.[7] have noted (though for a different catalyst than ours) that this is the last line to disappear during the saturation of polybutadiene.

The molecular masses of the polybutadiene stars were determined by gel permeation chromatography (GPC). The saturated materials were also checked by GPC, and the mass distributions of the protonated and deuteriated products were found to be very similar; the M_w values differed by less than 5%.

For each star a blend was prepared by mixing together approximately equal masses of the deuteriated and protonated materials in cyclohexane under reflux. This was done in a nitrogen atmosphere to prevent the polymers from being oxidized in solution, where they are particularly vulnerable to attack. Neutron measurements were made both for the blended sample and for a blank sample provided by a protonated material alone. The latter gives a measure of the incoherent scattering from the protons in the blended sample.

For an elastic scattering process the magnitude of the change in the wavevector of the neutron is

$$Q = \frac{4\pi}{\lambda} \sin \frac{1}{2}\theta \qquad (1)$$

where λ is the wavelength of the neutron and θ is the scattering angle. The neutron scattering measurements were made on the small-angle scattering spectrometer at the National Bureau of Standards at Gaithersburg[8] and on D17 at the Institut Laue-Langevin.[9] The measurements at the NBS were made with a sample–detector distance of 3.6 m and with incident wavelengths of 0.50 and 0.75 nm. These gave respective Q ranges of 0.14–1.6 nm^{-1} and 0.09–1.0 nm^{-1}. On D17 the detector was 2.8 m from the sample and was offset by an angle of 3° from the direction of the incident beam. The incident wavelength was 1.2 nm, giving a Q range of 0.13–0.9 nm^{-1}.

For both spectrometers the position-sensitive detector has a Cartesian grid of detecting elements. The scattering in the present

† Present address: Department of Physics, University of Warwick, Coventry CV4 7AL, U.K.
‡ Corporate Research Science Laboratories, Exxon Research and Engineering Company, Clinton Township, Annandale, NJ 08801.
§ Institut Laue-Langevin, 156X, 38042 Grenoble Cedex, France.
⊥ National Bureau of Standards, Gaithersburg, MD 20899.
‖ Los Alamos Neutron Scattering Center, Los Alamos National Laboratory, Los Alamos, NM 87545.

0024-9297/89/2222-0681$01.50/0

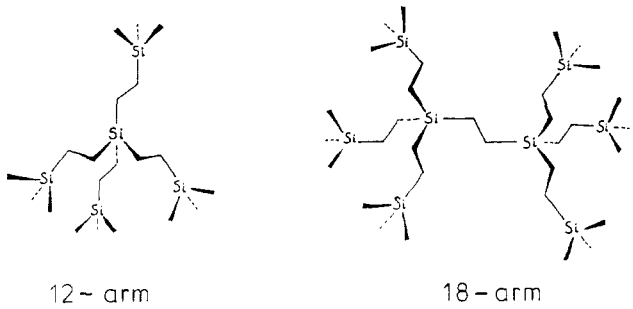

Figure 1. Chlorosilane cores of the 12- and 18-arm stars. Chlorine atoms (not shown) are attached to the outer silicon atoms and are replaced by linear polybutadiene chains to form a star molecule.

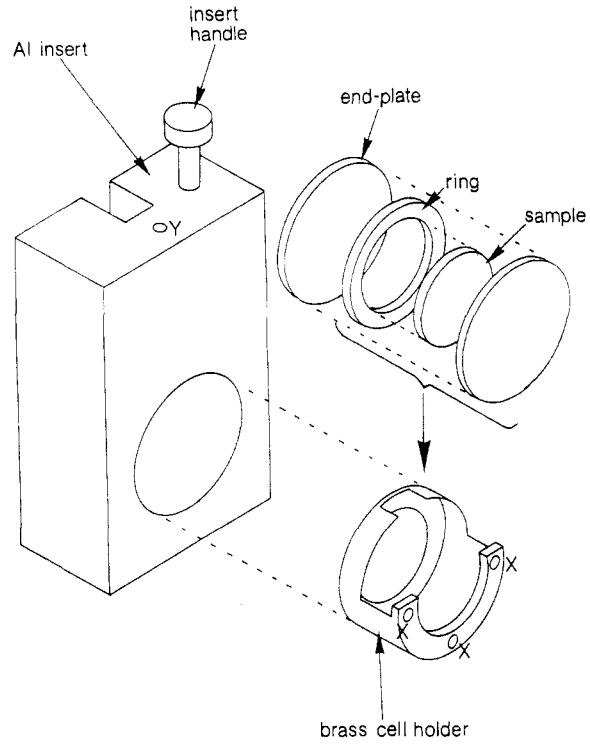

Figure 2. Cell and sample holder. The cell plates are secured by fiber-tipped screws inserted in the holes X. A platinum resistance thermometer is inserted in the hole Y in the Al insert.

experiment has azimuthal symmetry. The counts for the elements in a narrow annulus with the same Q value were therefore summed, giving the scattered neutron intensity for 72 Q values for the NBS spectrometer and 43 for D17.

Each sample was held in a glass cell consisting of two quartz end plates separated by a glass ring, giving a sample thickness of about 1 mm (Figure 2). The cell was mounted in a brass holder which could be conveniently placed in the heater (Figure 3). The latter held six samples, which could be maintained at the working temperature of 140 °C with an accuracy of about 0.5 °C. (The melting point of saturated polybutadiene is about 100 °C.)

For each sample, blend and blank, measurements were made of the scattered intensity $N(Q)$, normalized to a standard monitor count of the incident neutrons. The transmission ratio T, i.e., the fraction of neutrons passing through the sample without being scattered or absorbed, was also determined. In addition, $N(Q)$ was measured for an empty cell, to give the scattering from the end plates of the sample cell. The scattering was also measured for a sample of water. On the assumption that the scattering function of water is independent of Q over the range of the experiment, these data allow the neutron measurements from the polymer samples to be corrected for the variation of the sensitivity of the detector with Q. The background counts were measured by placing a sheet of cadmium close to the sample on the reactor side: they were so low as to be insignificant and will not be considered further.

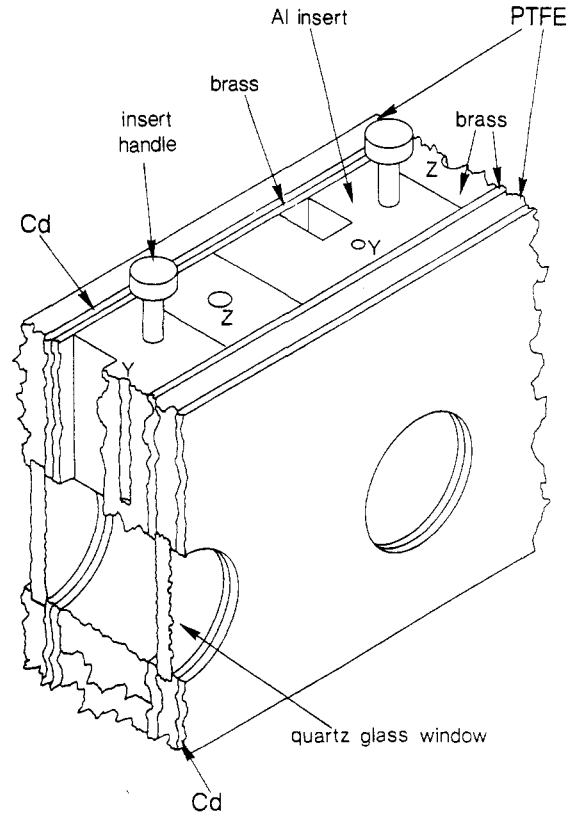

Figure 3. View of part of heater block from the beam side. The whole block can take six samples. Hole Y is for a platinum resistance thermometer and hole Z for a heater element. A further hole for a sensor element of the temperature controller is not shown.

The fraction of protons in the hydrogen nuclei of the blended sample is, to a good approximation,

$$\rho = 1 - cy \tag{2}$$

where c is the mass fraction of deuteriated polymer in the blend and y is the fraction of deuterons in the hydrogen nuclei of the deuteriated polymer. Ideally $y = {}^1/_4$; however, other workers[5,6] have found higher values due to exchange between some of the hydrogen atoms in the polybutadiene and deuterium.

For a fixed Q the coherent scattering cross-section of the deuteriated molecules is proportional to

$$I = \frac{1}{t_b}\left(\frac{N_b}{T_b} - \frac{N_{ec}}{T_{ec}}\right) - \frac{\rho}{t_h}\left(\frac{N_h}{T_h} - \frac{N_{ec}}{T_{ec}}\right) \tag{3}$$

where t is the sample thickness and the subscripts b, h, ec refer respectively to the blended sample, protonated sample, and empty cell. The transmission ratios were measured relative to that of the empty cell; thus, $T_{ec} = 1$.

It may be noted that the method of subtracting the incoherent background given in eq 3 is strictly correct only for very thin samples. For thicker samples, incoherent multiple scattering becomes important, and the incoherent intensity is proportional neither to the density of the protons in the sample nor to its thickness.[10] Thus an additional factor should multiply the second term on the right-hand side of eq 3. However, since the densities of the protons in the blended and protonated samples are not very different, and the two samples are of the same nominal thickness, this factor will be close to unity.

We may write (3) in the form

$$I = I_b - I_h - I_{ec} \tag{4}$$

where

$$I_b = N_b/t_bT_b \qquad I_h = \rho N_h/t_hT_h \qquad I_{ec} = N_{ec}\left(\frac{1}{t_b} - \frac{\rho}{t_h}\right) \tag{5}$$

For all the materials we studied, I_b varied from about $10I_h$ at the low-Q end of the measurements to about $2I_h$ at the high-Q end.

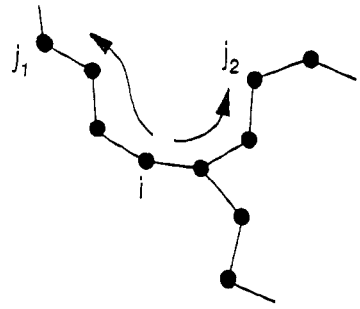

Figure 4. Probability distribution for the distance between monomers i and j_1 on the same arm is the same as that for the monomers i and j_2 on different arms.

The term I_{ec}, the net contribution to I due to the end plates, was very small, being always less than 1% of I_h.

We have made measurements on four linear molecules, five with $f = 3$, three with $f = 4$, five with $f = 12$, and one with $f = 18$, making a total of 18 in all.

Analysis of Data

For a molecule of squared radius of gyration $\langle S^2 \rangle$, the scattering function $I(Q)$ depends on the quantity $u = \langle S^2 \rangle Q^2$. Two common ways of analyzing the scattering data to obtain the value of $\langle S^2 \rangle$ are the Guinier and Zimm plots. The first is based on the equation $P(Q) = I(Q)/I(0) = \exp(-u/3)$ and the second on the equation $P(Q)^{-1} = 1 + u/3$. Both equations tend to the form $P(Q) = 1 - u/3$ as u becomes small compared to unity, which is the required expression for any scattering system. Initially we tried analyzing our data by each of these methods. However, they both proved unsatisfactory for the accuracy we required, giving discordant values for $\langle S^2 \rangle$, the Zimm values always being higher. The drawback is that both expressions are valid only in the range u small compared to unity, and the values obtained for $\langle S^2 \rangle$ depend on the range of Q values selected for the analysis. It tends to be a subjective decision as to when the experimental points start to depart from the linear relations postulated by the equations. On the other hand, if the selection is confined to those points for which the linear relation is clearly valid, then, for the range of Q values provided by both the spectrometers used, the number of acceptable experimental points was only about 5–10.

We therefore fitted the data to a more general expression, originally derived by Debye[11] for a linear polymer. It is based on a random-walk model and assumes, first, that the probability distribution for the distance r_{ij} between monomers i and j is a Gaussian proportional to $\exp(-r_{ij}^2/2\sigma^2)$ and, second, that σ^2 is proportional to the integer $|i - j|$. The calculation has been extended to branched polymers by Benoit,[12] on the assumption that the probability distribution is independent of whether or not the chain joining two monomers passes through a branch point—Figure 4. For a star molecule the Benoit expression for $P(Q)$ is

$$P_0(Q) = \frac{2}{x^2}\left\{\frac{x}{f} - \frac{1}{f}(1 - e^{-x}) + \frac{f-1}{2f}(1 - e^{-x})^2\right\} \quad (6)$$

$$x = \frac{\langle S^2 \rangle Q^2}{f g_0} \qquad g_0 = \frac{3f-2}{f^2} \quad (7)$$

The theoretical squared radius of gyration $\langle S^2 \rangle_0$ of the molecule may be calculated on the same assumption. The result is

$$\langle S^2 \rangle_0 = \frac{1}{6} g_0 C_\infty N_m a^2 \quad (8)$$

C_∞ is the characteristic ratio of polyethylene, N_m is the number of monomers in the backbone chains of the molecule, and a is the distance between successive monomers. For our material $N_m = M_w/14.0$, where M_w is the molecular weight of the polybutadiene molecule. (The denominator is increased from 13.5 to 14.0 in the expression for N_m due to the vinyl side groups mentioned above.)

We fitted the Benoit function $P_0(Q)$ to our experimental values $I(Q)$ by a weighted least-squares procedure that minimized χ^2, the mean-square value of the quantity (deviation/error) for the experimental points. The fit was obtained by varying two parameters, namely, the value of $\langle S^2 \rangle$ in (7) and that of a constant multiplying the function $P_0(Q)$. For most of the materials we were able to fit the Benoit function for a range of about 30–40 points with a value of χ between 1.0 and 1.3.

If the small term I_{ec} is neglected in eq 4, the quantities t_b, t_h, T_b, T_h, and ρ enter the expression for I as a single parameter

$$G = \rho \frac{t_b T_b}{t_h T_h} \quad (9)$$

Although the values of the transmissions, T_b and T_h, are known with adequate precision, there is some uncertainty in the values of the thicknesses, t_b and t_h, of the samples, due to the difficulty of filling the cells. Moreover, as mentioned above, not only is the value of $\rho = 1 - cy$ uncertain to some extent, but, due to multiple scattering, there is an additional factor (expected to be close to unity) multiplying the right-hand side of (9). Therefore the quantity G was varied to see if this would increase the range of Q points over which a fit to the Benoit function could be obtained. Some improvement was found, the resulting fit extending to almost the entire range of the data. The change in the value of G from its nominal value was of the order of 5%, and the resulting change in the value of $\langle S^2 \rangle$ was about 2 or 3%. The fact that the change in G was only 5% indicates that the effect of multiple scattering on the value of I was probably quite small. The values shown in Figure 5 and Table I are those given by the optimum G values.

The value of I was converted into an absolute macroscopic differential scattering cross section, $d\Sigma/d\Omega$, by measuring the scattering from standard samples with known macroscopic cross sections. Silica gel was used for this purpose at the NBS and distilled water at the ILL. In principle it is possible to check the molecular mass of the molecule from the value of $d\Sigma/d\Omega$ at $Q = 0$, since the latter is proportional to $y^2 M_w$. However, the uncertainty in y gives a large uncertainty in the value obtained for M_w.

In order to calculate $\langle S^2 \rangle_0$ we need the value of $C_\infty a^2$ in eq 8. The value we used was derived from the results for the linear molecules, for which we assume the measured value $\langle S^2 \rangle$ is equal to $\langle S^2 \rangle_0$. For linear molecules $g_0 = 1$, and we have

$$\langle S^2 \rangle_0 = \frac{C_\infty M_w a^2}{6 \times 14.0} \quad (10)$$

From the values of $\langle S^2 \rangle$ and M_w for the linear molecules we find

$$\left(\frac{C_\infty}{6 \times 14.0}\right)^{1/2} a = \frac{\langle S^2 \rangle_0^{1/2}}{M_w^{1/2}} = (0.0457 \pm 0.0012) \text{ nm} \quad (11)$$

which may be compared with the values 0.045 and 0.046 nm obtained by previous workers for polyethylene[13,14] and 0.050 ± 0.002 nm obtained for saturated polybutadiene.[15] The values of $\langle S^2 \rangle_0^{1/2}$ in Table I are thus given by

$$\langle S^2 \rangle_0^{1/2} \text{ (nm)} = 0.0457(g_0 M_w)^{1/2} \quad (12)$$

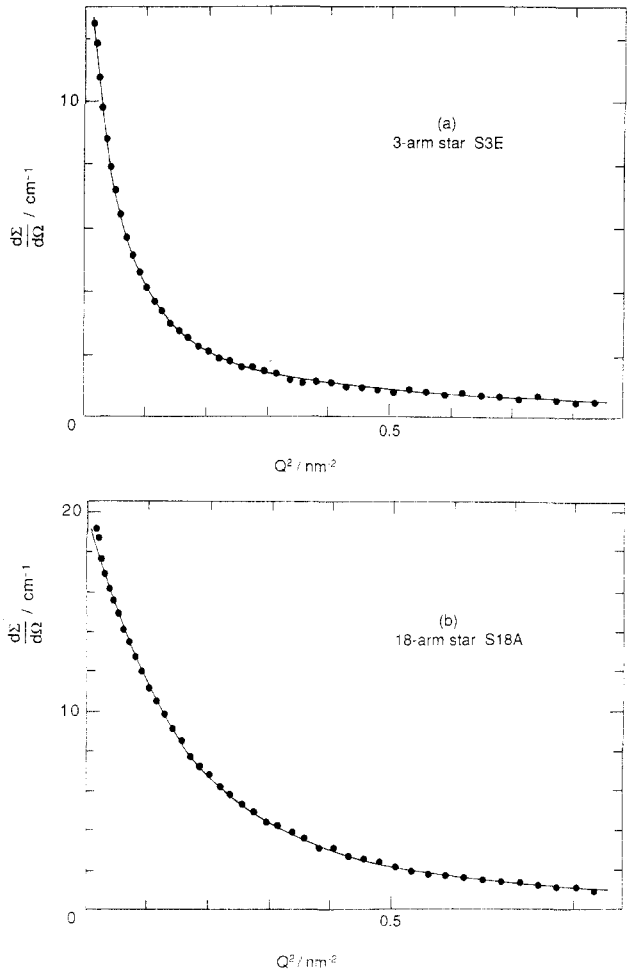

Figure 5. Representative experimental values of the macroscopic differential scattering cross section $d\Sigma/d\Omega$ versus Q^2. The curve through the points is the theoretical Benoit function for the fitted value of $\langle S^2 \rangle$. Part a shows the data for the 3-arm star S3E ($\langle S^2 \rangle^{1/2}$ = 7.65 nm) and part b the data for the 18-arm star S18A ($\langle S^2 \rangle^{1/2}$ = 4.29 nm).

In doing the least-squares analysis we feed the known value of the arm number f into the Benoit equation. However, it is of interest to see whether the neutron data are sufficiently accurate to determine the value of f. Accordingly, for some of the materials, we fed into the equation different f values and determined the value of χ for the best fit in each case. For nearly all the materials the value of χ at best fit has a lower value for the correct value of f than for any other integral value. For the 18-arm star the lowest value of the best-fit χ occurs for f = 20, which is reasonably close. Two representative sets of results are shown in Figure 6, where the best-fit χ is plotted against f for a 4-arm and a 12-arm star.

Discussion

We compare our results with various model calculations for star molecules. Daoud and Cotton[16] have calculated the swelling that may be expected for a molecule with f arms, based on a model in which each arm is a succession of blobs, with f blobs in successive spherical shells around the star point. Although the model is for star molecules in a good solvent, we may apply the basic idea to molecules in the melt. The prediction is that

$$\langle S^2 \rangle / \langle S^2 \rangle_0 \sim f^{-1} \tag{13}$$

with no dependence on molecular weight. This is clearly at variance with the results in Table I, in particular with the results for the 12-arm stars, where $\langle S^2 \rangle / \langle S^2 \rangle_0$ decreases with increasing molecular weight.

Table I
Experimental and Theoretical Values of the Radius of Gyration[a]

material	$M_w/10^3$	$\langle S^2 \rangle^{1/2}$, nm	$\langle S^2 \rangle_0^{1/2}$, nm	$\langle S \rangle^{1/2} - \langle S^2 \rangle_0^{1/2}$, nm	$\langle S^2 \rangle - \langle S^2 \rangle_0$, nm^2	$\langle S^2 \rangle / \langle S^2 \rangle_0$
linear						
S2A	10.8	4.70 ± 0.03	4.74	−0.04	−0.4	0.983
S2B	14.0	5.69 ± 0.03	5.40	0.29	3.2	1.110
S2C	32.1	8.46 ± 0.05	8.18	0.28	4.7	1.070
S2D	53.0	9.78 ± 0.05	10.51	−0.73	−14.8	0.866
3-arm						
S3A	5.46	3.02 ± 0.03	2.97	0.05	0.3	1.034
S3B	6.8	3.34 ± 0.03	3.32	0.02	0.1	1.012
S3C	8.9	3.93 ± 0.03	3.80	0.13	1.0	1.070
S3D	14.95	5.11 ± 0.04	4.92	0.19	1.9	1.079
S3E	39.8	7.65 ± 0.05	8.03	−0.38	−5.9	0.908
4-arm						
S4A	9.5	3.93 ± 0.03	3.52	0.41	3.1	1.247
S4B	22.3	5.86 ± 0.04	5.39	0.47	5.3	1.182
S4C	62.7	9.12 ± 0.05	9.04	0.08	1.5	1.018
12-arm						
S12A	8.95	2.95 ± 0.03	2.10	0.85	4.3	1.973
S12B	11.1	3.31 ± 0.03	2.34	0.97	5.5	2.001
S12C	28.3	4.55 ± 0.03	3.73	0.82	6.8	1.488
S12D	66.4	6.38 ± 0.03	5.72	0.66	13.9	1.244
S12E	186	10.51 ± 0.05	9.57	0.94	18.9	1.206
18-arm						
S18A	23.0	4.29 ± 0.04	2.77	1.52	10.7	2.399

[a] M_w is the molecular weight of the polybutadiene molecule; $\langle S^2 \rangle$ is the experimental value of the mean-squared radius of gyration given by the neutron scattering data; $\langle S^2 \rangle_0$ is the theoretical value of the mean-squared radius of gyration for a molecule with unswollen Gaussian conformation.

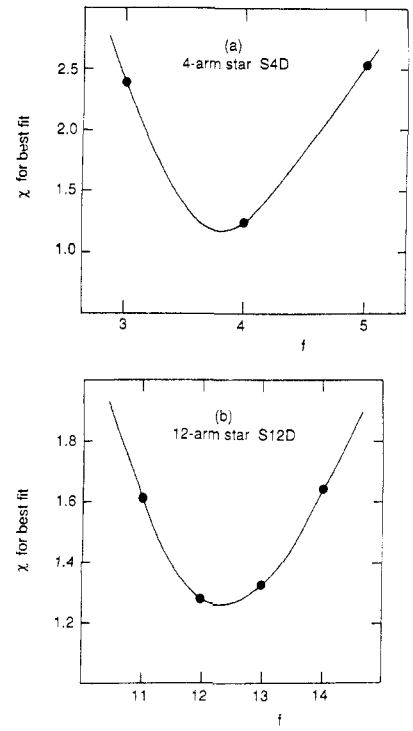

Figure 6. Variation of χ for the best fit of the experimental data to the Benoit scattering function with the value of the arm number f in the scattering function. Part a shows the variation for the 4-arm star S4A, and part b for the 12-arm star S12D. In both cases the best-fit χ has a minimum at values of f close to the actual arm number. The Benoit scattering function is defined (and hence χ may be calculated) for continuous values of f, but only integral values of f have physical meaning.

Several models for star polymers have been proposed which result in an expression for the radius of gyration of the form

$$\langle S^2 \rangle = \langle S^2 \rangle_0 + r^2(f) \tag{14}$$

where $r^2(f)$ is independent of molecular weight. This

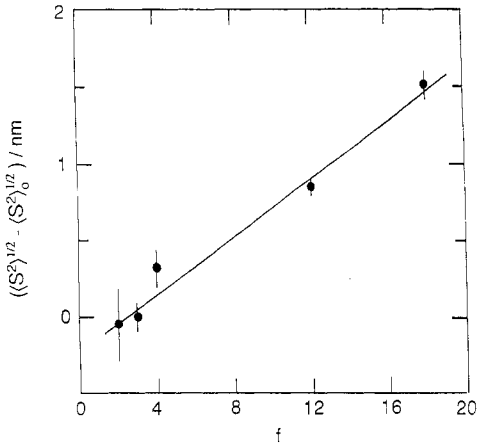

Figure 7. Mean value of $\langle S^2\rangle^{1/2} - \langle S^2\rangle_0^{1/2}$ for all molecules with same f value plotted against f. The straight line has a slope of 0.094 ± 0.008 nm.

general form is characteristic of models which introduce a non-Gaussian feature into the star center that affects only the monomers in the immediate neighborhood of the branch point. The wormlike model of Mansfield and Stockmayer[17] is one such example. It introduces rigid correlations between the arms close to the center, so that the onset of random-walk behavior is displaced a distance of the order of one persistence length from the star point. However, this model yields a negative value for $r^2(f)$; i.e., it predicts a contraction instead of a swelling, which is clearly in conflict with our results.

Another calculation based on this class of model is the recent Monte Carlo simulation of Huber et al.[18] In this work a specific center was employed, which closely modeled the actual chlorosilane core used in the synthesis of the star molecule. The rotational isomeric state method was then used to build up the whole star and to calculate the radius of gyration and the scattering function. Although eq 14 does not appear explicitly in ref 16, it is implied from the curves in Figure 6 of the first of the two papers cited in the reference. Our values of $\langle S^2\rangle - \langle S^2\rangle_0$ are listed in Table I and are clearly not independent of molecular weight for the 12-arm stars.

Ball[19] has calculated the swelling using the random phase approximation. In this model a repulsive potential is introduced at the center which acts to equalize the density of monomers within the star. He also obtains an expression like eq 14 and finds that the swelling is much smaller than that observed experimentally.

A different approach from those which yield expressions like eq 14 is to introduce a potential at the center which affects *all* the monomers of the star—not just those immediately adjacent to the star point. Boothroyd and Ball[20] have used a model with an impenetrable sphere at the center, with the arms diffusing outward from the core. They obtain an expression of the form

$$\langle S^2\rangle^{1/2} = \langle S^2\rangle_0^{1/2} + r(f) \qquad (15)$$

where the function $r(f)$ has no molecular weight dependence. This prediction does seem to give the best fit to our experimental results. The values of $\langle S^2\rangle^{1/2} - \langle S^2\rangle_0^{1/2}$ are listed in Table I, and for a fixed value of f, there appears to be no significant variation with molecular weight. For each value of f we have calculated the mean value of $\langle S^2\rangle^{1/2} - \langle S^2\rangle_0^{1/2}$ for all the molecules and plotted these values against f. The result, shown in Figure 7, is roughly a straight line with a slope of 0.094 ± 0.008 nm.

An obvious question that we have not yet addressed is whether the observed swelling is a trivial artifact arising from the structure of the molecule at the star center. The arms of the star are not joined at a point but are attached to an extended silicon core as shown in Figure 1. A rough calculation shows that the radius of the core is about 0.4 nm for the 4-arm stars and 1.1 and 1.6 nm for the 12- and 18-arm stars, respectively. Clearly the range of the hard-sphere potential is larger than that of the silicon core.

We have also checked to see whether the small amount of polydispersity of the samples modifies the scattering function sufficiently to account for the observed swelling.[21] However, the correction to the values of the radius of gyration for this effect is less than 0.1 nm.

Recent work[22] has indicated that segregation may occur in blends of deuteriated and protonated polymers. To check whether segregation is affecting our results, we have measured several blends of the material S12C with c values (eq 2) ranging from 0.25 to 0.75. The measurements were made with the LOQ spectrometer on ISIS at the Rutherford Appleton Laboratory. For the various blends, the values of the radius of gyration agreed to within 2%, and the relative values of $I(0)$ had the correct $c(1-c)$ dependence on composition expected for an unsegregated blend.[5] We conclude that segregation is not affecting our results.

Our overall conclusions are therefore (1) the Benoit scattering function gives an extremely good fit to the neutron scattering data, (2) the molecules are swollen with respect to a simple Gaussian conformation, and (3) the swelling is consistent with a model of an impenetrable core from which the arms of the star diffuse outward.

We have made a corresponding set of neutron measurements with the same set of materials in solution at the Θ temperature and in a good solvent. A report on this work will be given shortly.

Acknowledgment. We thank Prof. Klein of the Weizmann Institute for suggesting the present experiment, Dr. Heenan of the Rutherford Appleton Laboratory for assisting with the measurements on the LOQ spectrometer, Dr. Handley of the ICI Chemicals and Polymers Division for some independent measurements of the molecular weights, and Dr. Ball for illuminating discussions on the theory. J.C.H. and A.T.B. were supported by studentships from the Science and Engineering Research Council during the course of this work.

Registry No. Neutron, 12586-31-1.

References and Notes

(1) Flory, P. J. *J. Chem. Phys.* **1949**, *17*, 303.
(2) Kirste, R. G.; Kruse, W. A.; Schelten J. *Makromol. Chem.* **1973**, *162*, 299.
(3) Bauer, B. J.; Fetters, L. J. *Rubber Chem. Technol.* **1978**, *51*, 406.
(4) Rachapudy, H.; Smith, G.; Raju, V. R.; Graessley, W. W. *J. Polym. Sci., Polym. Phys. Ed.* **1979**, *17*, 1211.
(5) Tanzer, J. D.; Bartels, C. R.; Crist, B.; Graessley, W. W. *Macromolecules* **1984**, *17*, 2708.
(6) Klein, J.; Fletcher, D.; Fetters, L. J. *Faraday Symp. Chem. Soc.* **1983**, *18*, 159.
(7) Doi, Y.; Yano, A.; Soga, K.; Burfield, D. R. *Macromolecules* **1986**, *19*, 2409.
(8) Glinka, C. J.; Rowe, J. M.; LaRock, J. G. *J. Appl. Crystallogr.* **1986**, *19*, 427.
(9) Neutron Research Facilities at the ILL High Flux Reactor, 1986, p 38.
(10) O'Reilly, J. M.; Teegarden, D. M.; Wignall, G. D. *Macromolecules* **1985**, *18*, 2747.
(11) Debye, P. *J. Phys. Colloid Chem.* **1947**, *51*, 18.
(12) Benoit, H. *J. Polym. Sci.* **1953**, *11*, 507.
(13) Lieser, G.; Fischer, E. W.; Ibel, K. *J. Polym. Sci. Polym. Lett. Ed.* **1975**, *13*, 39.
(14) Schelten, J.; Ballard, D. G. H.; Wignall, G. D.; Longman, G.; Schmatz, W. *Polymer* **1976**, *17*, 751.
(15) Crist, B.; Tanzer, J. D.; Graessley, W. W. *J. Polym. Sci., Polym. Phys. Ed.* **1987**, *25*, 545.

(16) Daoud, M.; Cotton, J. P. *J. Phys. (Les Ulis, Fr.)* **1982**, *43*, 531.
(17) Mansfield, M. L.; Stockmayer, W. H. *Macromolecules* **1980**, *13*, 1713.
(18) Huber, K.; Burchard, W.; Bantle, S.; Fetters, L. J. *Polymer* **1987**, *28*, 1990, 1997.
(19) Ball, R. C., unpublished results.
(20) Boothroyd, A. T.; Ball, R. C., unpublished results.
(21) Boothroyd, A. T. *Polymer* **1988**, *29*, 1555.
(22) Bates, F. S.; Wignall, G. D.; Koehler, W. C. *Phys. Rev. Lett.* **1985**, *55*, 2415.

On the First-Order Transitions of Hydrogen-Bonded Liquid-Crystalline Poly(ester amides)

Shaul M. Aharoni

Engineered Materials Sector Research Laboratories, Allied-Signal Inc., Morristown, New Jersey 07960. *Received April 12, 1988; Revised Manuscript Received August 1, 1988*

ABSTRACT: The heats and entropies of 46 strictly alternating, hydrogen-bonded highly regular poly(ester amides) were obtained from the reproducible first-order endotherms in their DSC heating scans. The total

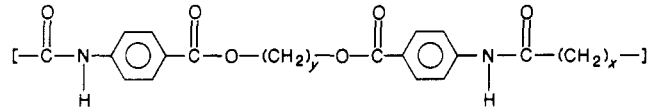

heats of transition, $\Delta H°_{tot}$, are in good agreement with literature values and group additivity calculations. All poly(ester amides) with $y = 2$, most of those with $y = 4$, and several with either very small x or $x = 20$ melt in a single step. The other ones, especially those with $8 \leq x \leq 14$ and $y = 3$ or $y = 5$, change from the crystalline to the isotropic state in several stages. The existence of three to four mesomorphic phases among the latter polymers is demonstrated by the number of transitions and the sizes of the heats of transition, as well as by hot-stage cross-polarized light microscopy. X-ray studies in a previous work[1] indicated at least one of the mesomorphic phases to be a smectic C or a twisted smectic C phase. Poly(ester amides) with $y = 3$ or $y = 5$ and $1 \leq x \leq 8$, as well as those with $y = 9$, exhibit two or three endotherms. Each of these endotherms is significantly smaller than $\Delta H°_{tot}$ or $\Delta H°_{m}$, the expected heat of melting, yet their sum is in good agreement with $\Delta H°_{tot}$. These polymers exhibit, hence, one or two mesomorphic phases. The specific nature of these phases for individual polymers is not known at present but microscopy observations lead us to believe that the first mesomorphic phase above the crystal/liquid crystal transition is a high-viscosity smectic phase. This phase converts to the isotropic melt when $x \leq 8$, or to a far lower viscosity smectic phase when $y = 3$ and $y = 5$ and $8 \leq x \leq 14$. At even higher temperature, the low-viscosity mesomorphic phase converts in one or two steps to an isotropic melt.

Introduction

In a recent publication[1] the preparation and characteristics of a new family of hydrogen-bonded liquid-crystalline poly(ester amides) were described. Here x stands

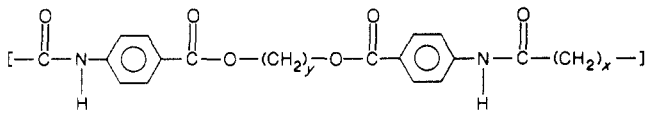

for the number of methylene groups between the amide residues and y is the number of methylene groups between the ester moieties. These poly(ester amides) will be denoted by their y and x values throughout this paper. The unique structural features of these polymers are their high regularity and strict alternation of two amide groups and two ester groups, the substitution of each aromatic ring in the para position by one amide and one ester group, and the fact that these reactive groups are pairwise connected by alkylene chains. The alkylene chains contain between one and 20 methylene groups. All amide residues are intermolecularly interacted with each other by hydrogen bonds (H-bonds) between adjacent chains. The H-bonds appear to exist over a broad temperature range, traversing the crystalline as well as the mesomorphic intervals.

Thermotropic liquid crystallinity was demonstrated in ref 1 by (a) the presence of multiple reproducible endotherms in the heating cycle of differential scanning calorimetry (DSC) scans, (b) the coexistence of sample mobility or spontaneous fluidity together with birefringence during observations in a hot-stage cross-polarized light microscope, and (c) the wide-angle X-ray diffraction (WAXD) patterns obtained from the crystalline polymers, their birefringent states, and isotropic melts, as well as from quick-quenched oriented and unoriented samples. The flat-plate X-ray patterns of oriented poly(ester amides) with $7 \leq x \leq 14$ were characterized by paucity of reflections and the complete absence of nonequatorial and nonmeridional reflections. Figure 1, for $y = 3$ and $x = 14$, is characteristic.

In this paper a study of some thermodynamic aspects of the first-order transitions of the poly(ester amides) will be presented. Experimentally, the investigation was conducted by DSC scans and cross-polarized light microscopy. In both procedures the heating and cooling rates were maintained at 10 K/min unless specified otherwise. The first-order transition points were all determined from the positions of the corresponding peaks in DSC scans[2,3] conducted at 10 K/min. The results of up to eight scans per polymer were averaged to obtain the reported temperature and heat of each transition. Throughout this paper all heats of transition, ΔH, are in units of kilojoule per mole. Crystallinity indices were obtained by conventional methods from WAXD powder diagrams. Details of the experimental procedures were published in ref 1.

Results and Discussion

DSC and cross-polarized light microscopy studies of the poly(ester amides) were presented in paper 1.[1] The per-

0024-9297/89/2222-0686$01.50/0